Eur Heart J Cardiovasc Imaging Abstracts Supplement, May 2016
doi:10.1093/ehjci/jew181

ORAL AB AGORA

1362

Cardiac Involvement in Patients With Different Rheumatic Disorders

S. Greulich[1]; D. Kitterer[2]; J. Latus[2]; J. Henes[3]; R. Kurmann[4]; S. Gloekler[4]; A. Wahl[4]; S. Buss[5]; H. Katus[5]; M. Bobbo[6]; M. Lombardi[7]; N. Braun[2]; M.D. Alscher[2]; U. Sechtem[1]; H. Mahrholdt[1]
[1]Division of Cardiology, Robert-Bosch-Medical Center Stuttgart, Germany; [2]Division of Nephrology, Robert-Bosch-Medical Center Stuttgart, Germany; [3]Abteilung Innere Medizin II, Universitätsklinik Tübingen, Germany; [4]Division of Cardiology, University Hospital (Inselspital) Bern, Switzerland; [5]Abteilung Innere Medizin III, Universitätsklinik Heidelberg, Germany; [6]Division of Cardiology, Institute for Maternal and Child Health, IRCCS Burlo Garofolo, Trieste, Italy; [7]Multimodality Cardiac Imaging Section, Policlinico San Donato, Milan, Italy

Purpose: There is much controversy about the prevalence of cardiac involvement in patients with rheumatic disorders. This is of importance, since consequences of cardiac involvement range from different treatment regimes to adverse outcomes. Consequently, our primary aim was to evaluate the prevalence of cardiac involvement in different forms of rheumatic disorders by CMR.
Methods: 297 patients underwent CMR. Cardiac involvement was defined by presence of late gadolinium enhancement (LGE). Patients with a history of myocardial infarction and/or prior revascularization procedure were excluded. Patients were further divided into 5 subgroups: (1) ANCA associated vasculitis, (2) non-ANCA associated vasculitis, (3) autoimmune connective tissue disorders, (4) arthritis, and (5) sarcoidosis.
Results: We enrolled n = 63 patients in the ANCA associated vasculitis group, 34 of them (54%) were LGE positive. LGE showed a non-ischemic pattern in 33 patients (97%), isolated ischemic LGE pattern was present in only 1 patient. The Non-ANCA associated vasculitis group consisted of 32 patients, in 7 patients (22%) LGE could be detected. LGE was non-ischemic in 6 patients (86%), isolated ischemic LGE was present in only 1 patient. In the group with connective tissue disorders 15 out of 110 patients (14%) showed LGE: Of these, 13 patients (87%) showed non-ischemic LGE, 2 patients isolated ischemic LGE, 2 patients had both non-ischemic and ischemic pattern. The Arthritis group consisted of 47 patients, in 10 of them (21%) LGE was detected. Non-ischemic LGE pattern was found in 8 patients (80%), ischemic LGE was present in 3 patients (30%), in one patient LGE-CMR revealed both LGE patterns. 45 patients were in the sarcoid group, 11 of them (24%) showed LGE: 8 patients had non-ischemic LGE (73%), 3 patients ischemic LGE (27%). Comparing prevalence of cardiac involvement in the five different rheumatic subgroups, the highest prevalence of cardiac involvement (54%) was detected in patients with ANCA-associated vasculitis. Conversely, in our cohort of autoimmune connective tissue disorders, LGE CMR revealed the lowest prevalence of cardiac involvement.
Conclusion: There is a wide variation in the prevalence of cardiac involvement in different groups with rheumatic disorders. In patients with ANCA associated vasculitis cardiac involvement seems to be common (54%), whereas patients with autoimmune connective tissue disorders seem to have a low prevalence of cardiac involvement (14%).

1366

Gender differences in the development of cardiac complications: a multicentric prospective study in a large cohort of thalassemia major patients

A. Meloni[1]; M.G. Neri[1]; P. Preziosi[2]; E. Grassedonio[3]; N. Schicchi[4]; P. Keilberg[1]; S. Pulini[5]; E. Facchini[6]; V. Positano[1]; A. Pepe[1]
[1]Fondazione G. Monasterio CNR-Regione Toscana, Pisa; [2]Policlinico "Casilino", Roma; [3]Ospedali Riuniti "Umberto I-Lancisi-Salesi", Ancona; [4]Arcispedale "S. Anna-Cona", Cona (FE); [5]Ospedale Civile "Spirito Santo", Pescara; [6]Policlinico "S. Orsola-Malpighi", Bologna; ITALY

Introduction: We aimed to prospectively assess if the male gender was associated with an higher risk of progressive cardiac iron accumulation, development of biventricular dysfunction and myocardial fibrosis assessed by CMR, and development of cardiac complications including heart failure (HF), arrhythmias and pulmonary hypertension (PH).
Methods: We considered 1711 TM patients (899 females, 31.09 ± 9.08 years), consecutively enrolled in the Myocardial Iron Overload in Thalassemia (MIOT) Network. Myocardial iron overload was assessed by the multislice multiecho T2* technique. Biventricular function was quantified by cine images. Late gadolinium enhancement (LGE) images were acquired to detect myocardial fibrosis.
Results: Although having a similar risk of accumulating iron, males showed a significant higher risk of developing cardiac dysfunction, heart failure, arrhythmias and cardiac complications globally considered (Table 1). Figure 1 shows the Kaplan-Meier curves for the outcomes for which the male sex was a significant prognosticator. Until 20-30 years of follow-up (FU) the two lines (male and female sex) were almost overlapping while after they clearly diverged.

	N(%) with positive outcome	Cox Regression	
		HR (95%CI)	P
Global heart T2*<20 ms:			
Female sex	253 (28.5)	Reference	0.470
Male sex	191 (23.2)	0.93 (0.77-1.27)	
Ventricular dysfunction:			
Female sex	179/771 (23.2)	Reference	<0.001
Male sex	262/721 (36.3)	1.84 (1.52-2.23)	
Myocardial fibrosis:			
Female sex	113/611 (18.5)	Reference	0.247
Male sex	106/585 (18.1)	1.17 (0.89-1.53)	
Heart failure:			
Female sex	56 (6.3)	Reference	<0.0001
Male sex	109 (13.3)	2.57 (1.86-3.55)	
Arrhythmias:			
Female sex	40 (4.5)	Reference	<0.0001
Male sex	64 (7.8)	2.17 (1.46-3.23)	
Pulmonary hypertension:			
Female sex	7 (0.8)	Reference	0.446
Male sex	7 (0.9)	1.51 (0.52-4.35)	
Cardiac complications:			
Female sex	96 (10.8)	Reference	<0.0001
Male sex	166 (20.2)	2.31 (1.79-2.97)	

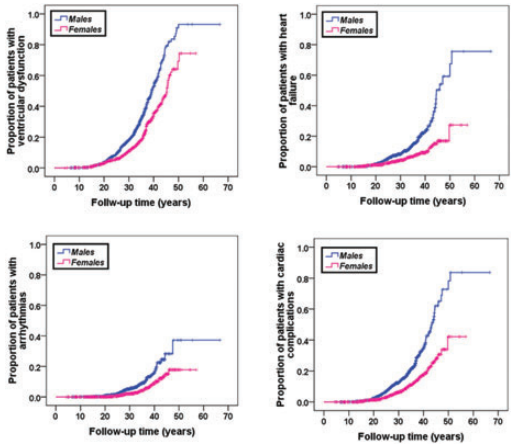

Patients were divided in two groups based on the FU duration. A significant gender-specific difference in the frequency of ventricular dysfunction and cardiac complications appeared for patients followed for at least 20 years. So, two subgroups of patients were identified: patients followed for less than 20 years and patients followed for more than 20 years. In the first subgroup males and females had a comparable risk of developing cardiac iron overload, ventricular dysfunction and cardiac complications. Conversely, if a FU longer than 20 years was considered, males exhibited a significant higher risk of having ventricular dysfunction, heart failure, arrhythmias, and cardiac complications.
Conclusion: Females seem to tolerate iron toxicity better, possibly as an effect of reduced sensitivity to chronic oxidative stress. According to the International Guidelines, TM patients should perform a complete cardiac evaluation every year. Our study suggested that in females older than 20 years the FU may be performed every 24 months, thus reducing health care costs.

1646

Comparison of T1-mapping, T2-weighted and contrast-enhanced cine imaging at 3.0T CMR for diagnostic oedema assessment in ST-segment elevation myocardial infarction

Sheraz A. Nazir; Abhishek Shetye; Jamal N. Khan; Anvesha Singh; Prathap Kanagala; Daniel Swarbrick; Gaurav Gulsin; Matthew Graham-Brown; Iain Squire; Anthony Gershlick; Gerry P. McCann

National Institute for Health Research (NIHR) Leicester Cardiovascular Biomedical Research Unit, University of Leicester, Leicester, UK

Background: Myocardial salvage index (MSI) derived using cardiac magnetic resonance (CMR) can be used to gauge success of reperfusion strategies; it remains a strong predictor of adverse remodeling and prognosis post STEMI. However, various limitations of sequences used to typically image myocardial oedema have made it challenging to achieve reliable AAR detection in the majority in clinical trials. Optimal detection of reversible myocardial injury could improve the reliability of MSI determination and its prognostic relevance.
Objective: To compare the robustness of myocardial oedema detection using T2-weighted short-tau inversion recovery (T2w-STIR), free-breathing motion-corrected (moco) T1-mapping and contrast-enhanced steady state free precession (CE-SSFP) sequences on 3.0T CMR in patients presenting with STEMI.
Methods: Forty-five patients underwent CMR 1-5 days following presentation with STEMI. AAR was quantified using semi-automatic thresholding on T2w-STIR and short-axis CE-SSFP cine images and resulting parametric colour maps from moco-T1 Modified Look Locker Inversion Recovery (MOLLI) sequences and compared using analysis of variance (ANOVA). Pearson's correlation coefficient was used to assess correlation. Inter-sequence agreement was assessed using the Bland-Altman method, coefficient of variation (CoV) and two-way mixed-effect intra-class correlation coefficient (ICC) for absolute agreement.
Results: Patient characteristics are presented in Table 1. AAR assessed using the three methods was not significantly different ($p = 0.988$) with excellent correlation and good agreement, although with wide limits of agreement (see Table 2). Correlation and agreement between AAR derived using moco-MOLLI and CE-SSFP were excellent. However, the diagnostic imaging rate obtained with T2w-STIR (76%) was poor compared with CE-SSFP (87%) and highest with moco-T1-mapping (98%), $p = 0.008$.
Conclusions: moco-T1-mapping using MOLLI may be the more robust than T2w-STIR and CE-SSFP for detecting reversible myocardial injury and determination of MSI for the prediction of functional recovery following STEMI. The poor diagnostic imaging rate of T2w-STIR may limit its usefulness in large clinical studies. CE-SSFP maybe a useful alternative to T2w-STIR for AAR detection where T1-mapping is not available. Our findings require validation in larger multi-centre studies.

Table 1: Patient Characteristics

Characteristic	n=45
Age (y)	56.6 ± 9.5
Male (n, %)	37, 82.2
Diabetes (n, %)	2, 4.4
Hypertension (n, %)	6, 13.3
IS (% LVM)	10.7 ± 7.5
LVEDVI (ml/m²)	89.9 ± 15.1
LVESVI (ml/m²)	51.8 ± 11.8
LVESVI (ml/m²)	56.0 ± 10.2
LVEF (%)	42.6 ± 7.7

BSA, body surface area; IS, infarct size; LV, left ventricular; LVEF, LV ejection fraction; LVEDVI, LV end-diastolic volume indexed to BSA; LVESVI, LV end-systolic volume indexed to BSA; LVM, LV mass; LVMI, LVM indexed to BSA

Table 2: Comparison of myocardial oedema assessed using T2w-STIR, T1-mapping and CE-SSFP sequences at 3.0T CMR

	T2w-STIR	T1-mapping	CE-SSFP	P-value
Diagnostic quality (n, %)	34, 75.6	44, 97.8	39, 86.7	**0.008**
AAR (g)	33.7 ± 14.3	33.9 ± 14.7	34.2 ± 15.6	0.988
	T2w-STIR v T1-mapping	T2w-STIR v CE-SSFP	T1-mapping v CE-SSFP	
R (Pearson's Correlation)	0.89 (p<0.001)	0.89 (p<0.001)	0.95 (p<0.001)	
Paired Mean difference (SD)	-1.56 (6.93)	-2.52 (7.37)	-0.61 (5.13)	
95% Limits of agreement	-15.1 to 12.0	-17.0 to 11.9	-10.7 to 9.4	
CoV (%)	20.0	21.2	15.0	
ICC	0.89	0.86	0.94	

AAR, area at risk; CE-SSFP, contrast-enhanced steady state free precession; CoV; Coefficient of Variation; ICC, Intra-class Correlation Coefficient; SD, standard deviation; T2w-STIR, T2-weighted short tau inversion recovery

ORAL AB AGORA | **ORAL AB AGORA** | **ORAL AB AGORA** | Friday May 13| 10:45—11:30

1375

Evaluation of Tissue Changes in Remote Noninfarcted Myocardium after Acute Myocardial Infarction using T1-mapping

P. Stefan Biesbroek, MD[1,2]; Raquel P. Amier, MD[1]; Paul F.A. Teunissen, MD[1]; Lourens F.H.J. Robbers[1]; Aernout M. Beek, MD, PhD[1]; Albert C. van Rossum, MD, PhD[1]; Mark B.M. Hofman, PhD[3]; Niels van Royen, MD, PhD[1]; Robin Nijveldt, MD, PhD[1]
[1]Department of Cardiology and Institute for Cardiovascular Research, VU University Medical Center, Amsterdam, The Netherlands; [2]Interuniversity Cardiology Institute of the Netherlands (ICIN), Utrecht, the Netherlands; [3]Department of Physics and Medical Technology, VU University Medical Center, the Netherlands

Background: Following acute myocardial infarction (MI) there is an extensive inflammatory reaction in infarcted myocardium. However, less is known about the inflammatory response in noninfarcted remote regions, and its role in cardiac remodelling. The present study assesses the temporal changes in T1-relaxation parameters (as markers of edema and cellularity) of the remote myocardium after acute MI, and determines its relationship with cardiac remodelling.
Methods: In this prospective study, 42 patients with acute MI treated with primary PCI were included and underwent CMR after 4-6 days and 3 months. Cine imaging, late gadolinium enhancement, and T1-mapping (MOLLI) was performed at 1.5T. T1-maps were acquired at the level of the infarcted area, before and 8 and 25-minutes after bolus (0.2 mmol/kg) injection of a gadolinium (Gd)-based contrast. T1 relaxation times were measured in the myocardial tissue opposite of the infarcted area. Gd-clearance rate was calculated by dividing the change in T1 between the 2 post-contrast time points by the time interval. Native T1 relaxation times were corrected for heart rate variability during data acquisition and were normalized to blood T1.
Results: Native T1 values of remote myocardium had significantly decreased from baseline to follow-up (997 ± 35 msec to 986 ± 27 msec, $p < 0.01$) (Figure 1). There were, however, no changes from baseline to follow-up in 8-min post-contrast T1 ($p = 0.48$), 25-min post-contrast T1 ($p = 0.16$), and Gd-clearance rate ($p = 0.95$). At baseline, remote native T1 values significantly differed between subgroups of patients, and were higher in patients with microvascular obstruction (MVO) ($p = 0.02$), an anterior MI ($p = 0.04$), absence of STsegment resolution (STR) (0.04), and large MI size ($p = 0.01$) (Figure 2). In a multivariable linear regression model, remote zone native T1 values at baseline were inversely associated with left ventricular ejection fraction (LVEF) at baseline (B: -0.08, $p < 0.01$), but were not associated with changes in LVEF or LV volumes.
Conclusion: In remote noninfarcted myocardium, a small change in native T1, but not in post-contrast T1 or Gd-clearance rate, was observed between baseline and 3 months after acute MI. Remote native T1 values at baseline were associated with markers of reperfusion injury and were independently associated with worse LVEF post-MI.

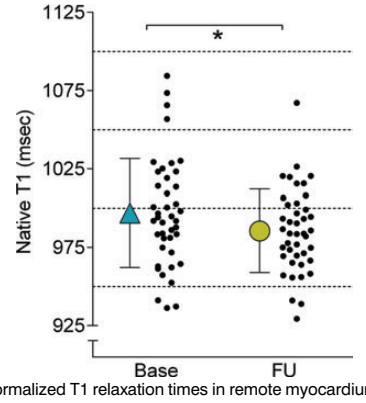

Figure 1. Native normalized T1 relaxation times in remote myocardium 4—6 days (base) and 3 months (FU) after MI.

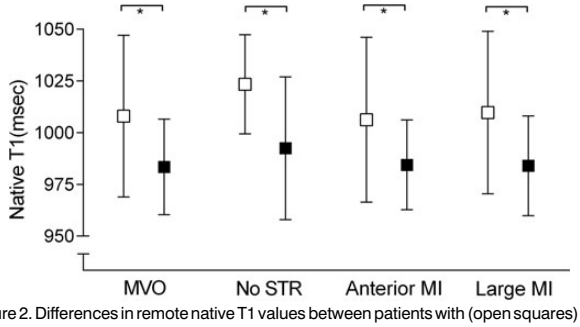

Figure 2. Differences in remote native T1 values between patients with (open squares) and without (black squares) MVO, anterior MI, no STR, and large MI.

ORAL AB AGORA | **ORAL AB AGORA** | **ORAL AB AGORA** | Friday May 13| 10:45—11:30

1377

Right ventricular long axis strain – The prognostic value of a novel parameter in non-ischemic dilated cardiomyopathy using standard cardiac magnetic resonance imaging

Nisha Arenja; Johannes H Riffel; Charly Noel Djiokou; Florian Andre; Thomas Fritz; Manuel Halder; Zelniker Thomas; Grigorios Korosoglou; Hugo A Katus; Sebastian J Buss
Department of Cardiology, Angiology and Pneumology, University of Heidelberg, Im Neuenheimer Feld 410, Heidelberg 69120, Germany

Background: Long axis strain (LAS) has been shown to be a fast assessable parameter for the analysis of left ventricular longitudinal function in cardiac magnetic resonance (CMR). However, the prognostic value of right ventricular long axis strain (RV-LAS) using CMR is unknown. This study investigates the association of RV-LAS with outcome in patients with non-ischemic dilated cardiomyopathy (DCM).
Methods: 350 consecutive patients with DCM were prospectively included and analyzed retrospectively. RV-LAS was assessed by measuring the length between the epicardial border of the left ventricular apex and the middle of a line connecting the origins of the tricuspidal valve leaflets in enddiastole and endsystole (figure 1). Values for RV-LAS were calculated according to the strain formula.
Results: The endpoint, a combination of cardiac death, heart transplantation, cardiac decompensation or sustained ventricular arrhythmias, occurred in 85 patients during a mean follow-up period of 3.8 $\pm$ 0.1 years. The mean values of RV-LAS were significant reduced in patients with endpoint (-10.6 $\pm$ 4.4 vs. -8.3 $\pm$ 3.9, p = <0.0001). On multivariate analysis, RV-LAS remained an independent predictor of the endpoint (HR 1.1, p = 0.004). ROC analysis yielded a RV-LAS criterion of -8.9% for the endpoint. Kaplan-Meier survival curves showed a reduced outcome in patients with RV-LAS $\leq$-8.9% (p < 0.0001).
Conclusion: Assessment of RV-LAS in CMR is an independent predictor of outcome in patients with DCM and offers incremental information beyond standard CMR parameters including LGE.

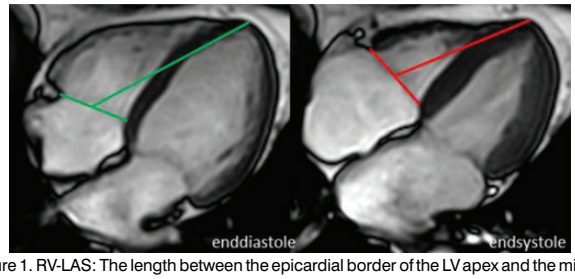

Figure 1. RV-LAS: The length between the epicardial border of the LV apex and the middle of a line connecting the origins of the tricuspidal valve leaflets was measured in both enddiastole and endsystole.

ORAL AB AGORA | **ORAL AB AGORA** | **ORAL AB AGORA** | Friday May 13| 10:45—11:30

1389

The role of the right ventricular insertion point in heart failure patients with preserved ejection fraction: Insights from a cardiovascular magnetic resonance study

Andreas A. Kammerlander; Marianne L. Schwaiger; Franz Duca; Stefan Aschauer; Beatrice A. Marzluf; Caroline Zotter-Tufaro; Daniel Dalos; Stefan Pfaffenberger; Diana Bonderman; Julia Mascherbauer
Department of Cardiology, Medical University of Vienna, Austria

Background: In pulmonary hypertension (PH), increased afterload for the right ventricle (RV) is reported to induce fibrosis at the RV insertion point (RVIP), detectable by cardiac magnetic resonance (CMR) using late gadolinium enhancement (LGE). In contrast to LGE imaging, T1-mapping, a new CMR technique, allows quantitative assessment of myocardial native T1 times and extracellular volume (ECV). However, the role of T1-mapping of the RVIP in humans is unknown and the prognostic value has never been investigated.
Methods: We investigated 116 patients with heart failure and preserved ejection fraction (HFpEF), a patient population frequently suffering from PH, who underwent CMR including T1-mapping. Of these, 100 (86%) underwent right heart catheterization (RHC) for hemodynamic assessment. Native T1-times were measured at the anterior and inferior RVIP and ECV was calculated.
Patients were followed for 21 $\pm$ 18 months and the prognostic value of T1-mapping of the RVIPs was investigated by Cox-regression analysis.
Results: A total of 82% suffered from PH (mean pulmonary artery pressure, mPAP, $\geq$25mmHg). In 30%, LGE was detectable at the anterior RVIP, which was associated with higher mPAP as compared to patients without LGE (39 $\pm$ 13mmHg vs. 32 $\pm$ 9mmHg, p = 0.045), however, this was not seen for the inferior RVIP (34 $\pm$ 11mmHg vs. 31 $\pm$ 10mmHg, p = 0.118), where in 77% of patients LGE was present.
Native T1-times were 987 $\pm$ 78ms at the anterior and 1017 $\pm$ 89ms at the inferior RVIP and ECV was 32 $\pm$ 6% and 35 $\pm$ 7%, respectively. There was a significant correlation between mPAP and native T1 times as well as ECV of the anterior RVIP (r = 0.354, p < 0.001 and r = 0.248, p = 0.038) and the inferior RVIP (r = 0.248, p = 0.026 and r = 0.289, p = 0.015).
In total, 23% experienced a cardiovascular event. By Kaplan-Meier analysis, LGE was significantly associated with reduced survival when present at the anterior RVIP (log-rank, p = 0.011) but not at the inferior RVIP (log-rank, p = 0.207).
By multivariable Cox-regression, native T1-times at the anterior, but not the inferior, RVIP above the median were significantly associated with outcome (p = 0.037), even after adjusting for age, atrial fibrillation, diabetes, NT-proBNP levels, RV size and function, and presence of LGE at the anterior RVIP.
Conclusion: T1-mapping at the anterior RVIP provides new insights in the pathological processes in HFpEF patients and might detect alterations at early stages in these patients. Additionally, it is a predictor of outcome.

ORAL AB AGORA | **ORAL AB AGORA** | **ORAL AB AGORA** | Friday May 13| 10:45—11:30

1398

Myocardial fibrosis associates with B-type natriuretic peptide levels and outcomes more than wall stress

Aatif Sayeed; Yaron Fridman, MD; Brianne Hackman, MD; Ajay Kadakkal, MD; Maren Maanja; Hussein Abu Daya, MD; Timothy C. Wong, MD, MS; Erik B. Schelbert, MD, MS
UPMC Cardiovascular Magnetic Resonance Center, Heart and Vascular Institute, Pittsburgh, PA, USA

Background: B-type natriuretic peptide (BNP) is a nonspecific cardiac risk marker attributed to hemodynamic wall stress that strongly associates with adverse outcomes, but whether myocardial fibrosis (MF) is more strongly associated with both BNP and risk than wall stress is uncertain. Such data might demonstrate MF as a novel etiology of BNP elevation and further promote the emerging paradigm of MF as a therapeutic target in cardiomyopathy and heart failure.
Methods: We measured MF with histologically validated extracellular volume fraction (ECV) measures in 1176 consecutive adult individuals referred for clinical cardiovascular magnetic resonance (CMR). Linear regression quantified associations with log transformed BNP. Among those at risk with elevated BNP ($\geq$100 pg/mL), Cox regression models quantified associations with the combined endpoint of all-cause mortality or hospitalization for heart failure (HHF) using a standardized definition, blinded to ECV and wall stress data. All multivariable models (linear or Cox) adjusted for demographics, EF and volumes, body mass, renal function, atrial fibrillation, mitral regurgitation, ischemic cardiomyopathy, and myocardial infarction size.
Results: Median age was 56 years (IQR 44-66). Median ECV was 27.6 (IQR 25.5-30.7%). Both ECV and wall stress associated with log BNP (p < 0.001) in univariable linear regression models, but ECV was more strongly associated (t value 17.2 vs. 15.5). In multivariable linear regression models, ECV remained strongly associated with log BNP (t value 10.6, p < 0.001), whereas wall stress was no longer associated with log BNP (t value 0.7, p = 0.51). In 497 patients with BNP $\geq$ 100 pg/mL, 103 events occurred (43 HHF and 78 deaths including 16 deaths after HHF) over a median of 2.3 years. Wall stress did not associate with outcomes. In contrast, ECV was the variable most strongly associated with adverse events (HR 1.36 95%CI 1.15-1.61) for every 5% increase in multivariable Cox models.
Conclusion: Myocardial fibrosis (MF) is more strongly associated with BNP than wall stress. In those with elevated BNP, ECV was robustly associated with outcomes but wall stress was not. These data suggest that MF is a key mediator of cardiomyopathy and vulnerability. Since MF is known to be reversible, MF may be a promising therapeutic target in heart failure and cardiomyopathy.

ORAL AB AGORA | **ORAL AB AGORA** | **ORAL AB AGORA** | Friday May 13| 10:45—11:30

1478

Prognostic Value of Pulmonary Blood Volume by Contrast-Enhanced Magnetic Resonance Imaging in Heart Failure Outpatients – The PROVE-HF Study

F. Ricci, MD; A. Barison, MD, PhD; G. Todiere, MD; R. Gaeta, MD, PhD; S. Galllina, MD, PhD; M. Emdin, MD, PhD; R. De Caterina, MD, PhD; G.D. Aquaro, MD
Institute of Cardiology, University "G. d'Annunzio", Chieti, Italy; G. Monasterio Foundation, MRI-laboratory, Pisa, Italy

Background: In patients with heart failure (HF) early diagnosis of subclinical congestion is key to ensure prompt and effective treatment, and to prevent recurrent hospitalizations. Pulmonary blood volume (PBV) is a novel magnetic resonance (MRI) tool for the quantitative evaluation of pulmonary congestion.
Purpose: To prospectively assess the prognostic value of PBV in a cohort of HF outpatients.
Methods: Forty-four consecutive patients (34 men, 60 $\pm$ 12 years) and 31 age- and sex-matched healthy controls underwent contrast-enhanced cardiac MR. PBV was calculated as the product of stroke volume and number of cardiac cycles for an intravenous bolus

of gadolinium contrast to pass through the pulmonary circulation, as determined by first-pass perfusion imaging.

Results: As compared to healthy controls, chronic HF outpatients showed significantly higher PBV index (PBVI, 317 $\pm$ 112 vs. 379 $\pm$ 146, ml/m2, p = 0.03) and pulmonary transit time (PTT, 6.6 $\pm$ 1.8 vs. 8.4 $\pm$ 2.9 sec, p = 0.004). PBVI was significantly associated with echocardiographic indices of diastolic dysfunctioN. Namely, PBVI showed a moderate positive correlation with tissue-Doppler E/E' ratio (R2 = 0.391, P < 0.001) and systolic pulmonary artery pressure, as assessed by CW-Doppler (R2 = 0.255, P < 0.001).During a median follow-up period of 39 $\pm$ 20 months, 13 patients (29%) reached the composite end-point of cardiovascular death, HF hospitalization or sustained ventricular arrhythmias/appropriate ICD intervention. Using a cut-off point of PBVI >541 ml/m2, corresponding to 2SD above the mean of healthy controls, Kaplan-Meier event-free survival rates were significantly higher in patients below (81%) as compared with patients above (14%) this cut-off (P < 0,001). On multivariate analysis PBVI was the only independent predictor of the composite end-point (HR 8.3- 95% CI: 2.01-35.66; p = 0.004).

Conclusions: PBVI is a novel approach to quantitatively determine pulmonary intravascular blood pool and may be used to evaluate the severity of pulmonary congestion in HF patients undergoing cardiac MRI examination.

ORAL AB AGORA | **ORAL AB AGORA** | **ORAL AB AGORA** | Friday May 13| 10:45—11:30

1370

Magnetic Resonance Adenosine Perfusion Imaging as Gatekeeper of Invasive Coronary

Peter Bernhardt, MD; Dominik Buckert, MD; Nils Dyckmanns, MD; Wolfgang Rottbauer, MD

Department of Internal Medicine II, University of Ulm, Ulm, Germany

Background: Current guidelines for the diagnosis and management of patients with stable coronary artery disease (CAD) strongly support the performance of non-invasive imaging techniques for the detection of myocardial ischemia prior to revascularization procedures. This recommendation originates from the strong evidence base showing the lack of prognostic benefit from percutaneous coronary interventions (PCI) over optimal medical therapy in patients without verification of myocardial ischemia. On the other hand, it could be demonstrated that patients with functionally significant coronary artery stenoses do benefit from revascularization. Cardiac magnetic resonance imaging (CMR) has emerged to be a diagnostic modality of choice for the detection of myocardial ischemia with high sensitivity and specificity. We therefore designed this prospective and randomized trial to compare a CMR-driven vs. angiography-driven management of patients with stable CAD and pathologic stress ECG concerning major cardiac endpoints, futile angiographies and quality of life.

Methods: Consecutive patients suspicious of initial manifestation or progress of CAD were prospectively enrolled in this study. After obtainment of written consent, subjects were randomized 1:1 into two groups. Group I directly underwent coronary angiography. PCI was performed in case of $\geq$70% stenosis in a coronary vessel with $\geq$2 mm diameter. Group II underwent contrast-enhanced (Dotarem, Guerbet, France) adenosine-perfusion CMR at 3 Tesla. Patients that exhibited reversible ischemia were then sent to PCI. All patients received optimal medical therapy.

After sample size estimation and power analysis, follow-up was planned to be 3 years for every patient.

Primary endpoint was defined as cardiac death and non-fatal myocardial infarction. Secondary endpoints were number of coronary angiographies with and without PCI and change in symptoms/quality of life. Symptoms were objectified by the Seattle Angina Questionnaire (SAQ) at baseline and after each year of follow-up.

Results: After randomization, group I consisted of 101 patients, 93 of these patients were treated according to protocol. In group II, 95 out of 99 patients received the initially planned treatment. In group I, there 50 (53.8%) coronary angiographies revealed no obstructive CAD. The other 43 (46.2%) subjects were treated with PCI. In the CMR group, 68 (71.6%) patients did not exhibit reversible ischemia and were thus treated conservatively. The other 27 (28.4%) patients with reversible ischemia were sent to PCI. SAQs showed no significant baseline difference between both groups. One year results are expected in January 2016.

Conclusion: This is a randomized and prospective clinical trial with three-years follow-up period, which will prove whether a CMR-driven management of patients with stable CAD is non-inferior compared to primary coronary angiography regarding hard end-point as myocardial death or non-fatal myocardial infarction and quality of life assessed by the SAQ. One year follow-up data will be available for presentation during the EuroCMR meeting 2016.

ORAL AB AGORA | **ORAL AB AGORA** | **ORAL AB AGORA** | Friday May 13| 16:10—16:55

1509

Influence of non-invasive hemodynamic CMR parameters on maximal exercise capacity in surgically untreated patients with Ebstein's anomaly

Christian Meierhofer; Andreas Kühn; Nerejda Shehu; Jan Müller; Heiko Stern; Peter Ewert ; Sohrab Fratz; Manfred Vogt

Pediatric Cardiology and Congenital Heart Disease, Deutsches Herzzentrum München, Technical University of Munich, Munich

Introduction: Ebstein's anomaly is often associated with RV dysfunction. Data on RV function in surgically untreated patients are however rare. Since a good quality of life correlates with a good exercise capacity in daily life, we investigated non-invasive quantitative data derived from cardiovascular magnetic resonance (CMR) and its impact on maximal exercise capacity in patients with surgically untreated Ebstein's anomaly.

Methods: We investigated 54 unoperated patients with Ebstein's anomaly, age 5 to 69 years (median 30 years) and examined these patients with CMR and cardiopulmonary exercise testing (CPET). We compared seventeen CMR parameters with CPET parameters. We performed univariate and multivariate analysis with the focus on the maximal exercise capacity in these patients. For the maximal exercise capacity peak oxygen uptake as the percentage of normal (peakVO2%) was selected. The following CMR volume and flow parameters were correlated to peakVO2%. Both right and left ventricular ejection fraction (RVEF and LVEF), the indexed enddiastolic and endsystolic volumes (RVEDVi, RVESVi, LVEDVi and LVESVi) as well as the indexed stroke volumes (RVSVi and LVSVi), the total normalized right and left heart volumes (volume of the atrium and the ventricle together) as well as the total right to left heart volume ratio (R/L-ratio). Indexed flow data as the antegrade (PA ante, Aorta ante) and the indexed net flow (PA netto, Aorta netto) in the pulmonary artery and the aorta as well as its normalized values on heart rate (CI-PA, CI-Aorta) were used.

Results: RVEF (r2 0.2788), PA netto (r2 0.2330), and PA ante (r2 0.1912) showed the best correlation with peakVO2% (all p < 0.001). Further significant linear correlation could also be demonstrated with CI-PA, LVEF, LVSVi, Aorta netto, RVESVi and Aorta ante. All other parameters did not show a significant correlation with peakVO2%. Multivariate analysis for RVEF and PA netto revealed a r2 of 0.4350.

Conclusions: CMR parameters reflecting cardiac function as RVEF and LVEF and flow data of cardiac forward flow best correlate to peakVO2%. The evaluation of the indexed net flow in the pulmonary artery and the overall function of the right ventricle (RVEF) best predicts the maximal exercise capacity in patients with Ebstein's anomaly.

ORAL AB AGORA | **ORAL AB AGORA** | **ORAL AB AGORA** | Friday May 13| 16:10—16:55

1356

Proximal aortic stiffening in Turner patients is more pronounced in the presence of a bicuspid valve. A segmental functional MRI study

Daniel G.H. Devos[1]; Katya De Groote[2]; Danilo Babin[3]; Laurent Demulier[4]; Yves Taeymans[4]; Jos J. Westenberg[5]; Luc Van Bortel[6]; Patrick Segers[7]; Eric Achten[1]; Jean De Schepper[8]; Ernst Rietzschel[9]

[1]Department of Radiology, MRI (-1K12), Ghent University Hospital, De Pintelaan 185, B-9000, Gent, Belgium; [2]Division of Pediatric Cardiology, Department of Pediatrics and Turner Clinic, Ghent University Hospital, Gent, Belgium; [3]Telecommunications and Information Processing, TELIN-IPI-iMinds, Faculty of Engineering and Architecture, Ghent University, Belgium; [4]Department of Cardiology, Ghent University Hospital, Ghent, Belgium; [5]Department of Radiology, Leiden University Medical Center, Leiden, The Netherlands; [6]Heymans Institute of Pharmacology, Ghent University, Ghent, Belgium; [7]IBiTech-bioMMeda, Ghent University, Ghent, Belgium; [8]Division of Pediatric Endocrinology, Department of Pediatrics and Turner Clinic, Ghent University Hospital, Gent, Belgium; [9]Department of Cardiology, Ghent University & Ghent University Hospital, De Pintelaan 185, B-9000, Gent, Belgium

Objective: To study structural and functional segmental aortic properties in Turner syndrome (TS) patients.

Methods: Aortic abnormalities contribute to increased morbidity and mortality of women with Turner syndrome. MRI allows segmental study of aortic elastic properties.

Using MRI, we performed pulse wave velocity (PWV) and distensibility measurements of the thoracic and abdominal aorta in 55 TS-patients, aged 13 to 59 years, and in a control population (n = 31; aged 21 to 58 years). We investigated the contribution of TS on aortic stiffness in our entire cohort, in aortic valve-morphology subgroups, and in the younger and older subgroups.

Results: Compared to controls, TS patients had higher PWV of the entire aorta (F = 7.3; p = 0.009) and thoracic aorta (TA-PWV; F = 10.5; p = 0.002), but not of the abdominal aorta (F = 0.3; p = 0.619). Ascending aortic (AA) diameters (but not more distal aortic diameters) were also significantly larger (F = 4.2; p = 0.043). No differences in distensibility were found. The increase in TA-PWV and AA diameters was more pronounced in bicuspid compared to tricuspid TS patients. Similarly, bicuspid TS patients also showed a decreased proximal aortic distensibility. In exploratory analyses, the observed proximal aortic stiffening and dilatation were largely similar when comparing younger and older TS patients.

Conclusion: Turner patients exhibit a predominant stiffening and dilatation of the proximal aorta, more pronounced when their aortic valve is bicuspid. These abnormalities are present at an early age, suggesting an aortic wall disease inherent to the TS, and only limited effect of accelerated ageing in the young adult Turner patient.

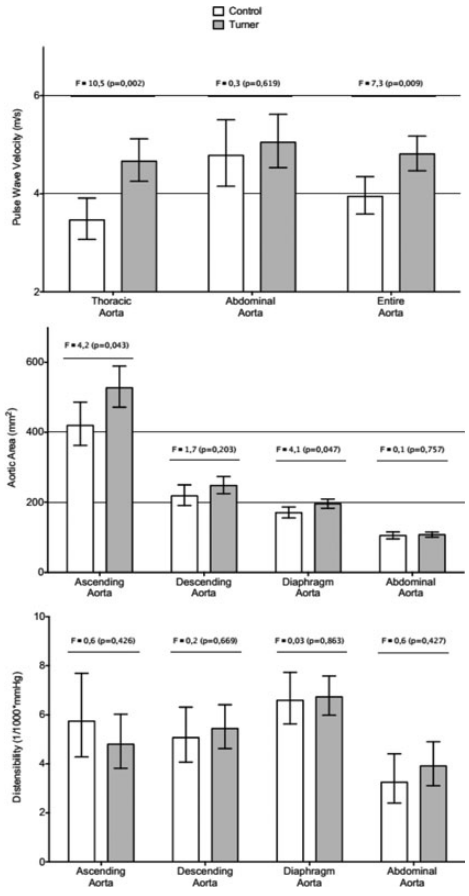

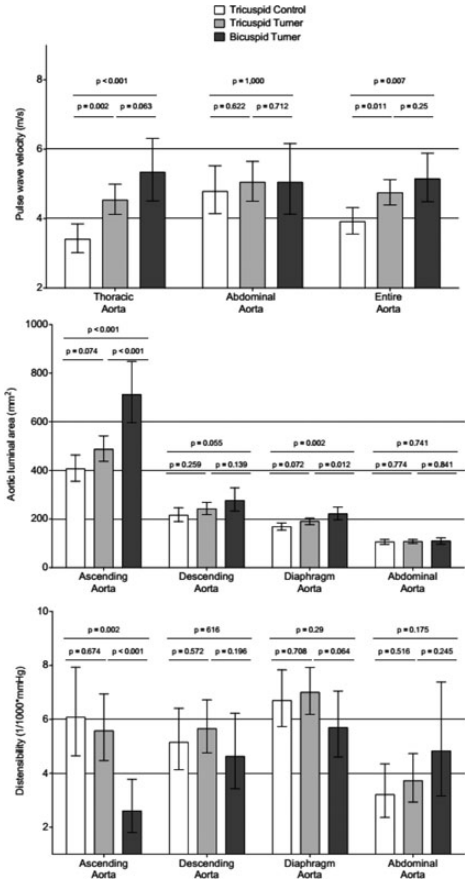

ORAL AB AGORA | **ORAL AB AGORA** | **ORAL AB AGORA** | Friday May 13| 16:10—16:55

1503

Flow pattern and vascular distensibility of the pulmonary arteries in patients after repair of tetralogy of Fallot. Insights from 4D flow CMR

Beate Ruecker; Julia Geiger; Malek Makki; Barbara Burkhardt; Christian J. Kellenberger; Emanuela R. Valsangiacomo Buechel

Paediatric Heart Centre, University Childreńs Hospital Zurich, Steinwiesstrasse 75, 8032 Zurich, Switzerland

Objectives: Pulmonary regurgitation is a frequent sequela after repair of tetralogy of Fallot (TOF). The regurgitant flow may lead to changes in the flow profile and in size and distensibility of the pulmonary arteries (Pas).
We sought to assess Pa flow and distensibility in TOF patients (pts) by cardiac magnetic resonance (CMR) and to correlate them with the flow patterns provided by 4D flow CMR.
Methods: 18 TOF pts (mean age 28 $\pm$ 11yrs, weight 63 $\pm$ 12 kg) and 9 control subjects (age 17 $\pm$ 7yrs, weight 63 $\pm$ 24kg) underwent CMR. 2D Phase-contrast (PC) images were acquired through-plane in the main (MPA), right (RPA) and left pulmonary artery (LPA). A 4D PC dataset was acquired covering all the great arteries. Vessel areas and quantitative flow were measured on the 2D PC images. The flow patterns in MPA, RPA and LPA were qualitatively assessed for presence of helix or vortex on the reconstructed 4D images. Flow parameters, size and distensibility of the Pas were compared between TOF pts and controls and in the TOF group between RPA and LPA with regard to helix/vortex.
Results: In TOF pts, MPA mean regurgitant fraction (RF) was 25 $\pm$ 17%. Compared to controls, both Pas were larger and distensibility was higher in LPA (p 0.048) but not in RPA. RF was greater in LPA than in RPA (29 $\pm$ 19% vs 16 $\pm$ 14%, p 0.001) and LPA area was larger than RPA area (316 $\pm$ 134 vs 257 $\pm$ 116 mm2/m2, p 0.0342). LPA net flow was lower than RPA net flow (p 0.0005). Distensibility was similar in LPA and RPA and significantly correlated with RF, regurgitant flow and minimum area in both Pas branches.
By 4D flow, vortex was observed in the LPA in 72% (13/18) of TOF pts, but not in normals. Helical flow was present in 44% (8/18) of pts and in 11% (1/9) of normals. Presence of vortex in the LPA was independent from any other parameter; LPA helix was more frequent in pts with higher distensibility (p 0.04).
RPA presented helical flow in 77% (14/18) of TOF pts and in 55% (5/9) of controls. Vortex was only detected in 11% (2/18) of TOF pts. RPA helical flow was not correlated to other parameters.
Conclusion: In pts after TOF repair, Pas size and distensibility are mainly determined by the amount of regurgitant flow and less by specific flow patterns, such as vortex or helix. Characteristic flow patterns are found in LPA and RPA, which seem to be more related to the geometry of the pulmonary bifurcation and its branches than to quantitative flow parameters.

ORAL AB AGORA | **ORAL AB AGORA** | **ORAL AB AGORA** | Friday May 13| 16:10—16:55

1516

Myocardial deformation characteristics of the systemic right ventricle after atrial switch operation for transposition of the great arteries

B.E.U. Burkhardt[1,2]; C.J. Kellenberger[2,3]; J. Geiger[2,3]; B. Ruecker[1,2]; E.R. Valsangiacomo Buechel[1,2]

[1]Children's Heart Center, University Children's Hospital Zurich, Switzerland; [2]Children's Research Center, University Children's Hospital Zurich, Switzerland; [3]Diagnostic Imaging, University Children's Hospital Zurich, Switzerland

Introduction: The atrial switch operation (Senning) has been the main surgical repair technique for d-transposition of the great arteries for many years. The Senning procedure results in a subsystemic morphologic right ventricle (RV) and a subpulmonary morphologic left ventricle (LV). This can be regarded as a model for the effects of long-term pressure overload on the RV, and of ultimately decreased afterload on the LV. We sought to determine the impact of these chronically altered loading conditions on the myocardial deformation of the RV and LV.
Methods: 26 patients after Senning (age 28.4 $\pm$ 7.5y) and 18 normal controls (age 22.2 $\pm$ 11.4y; p $=$ 0.034) underwent cardiac magnetic resonance (CMR) imaging. 2D SSFP cine images were acquired in an horizontal long axis and in a short axis covering both ventricles and post-processed with a feature tracking software (TomTec 2D CPA). Global circumferential strain was measured on a short axis mid-ventricular slice. Global longitudinal strain was measured in a long axis, separately for each ventricle.
Results: When comparing RV in either position, subsystemic circumferential strain was higher than subpulmonary circumferential strain (-16.1 $\pm$ 2.9% vs. -13.1 $\pm$ 4.3%; p $<$ 0.01), and subsystemic longitudinal strain was lower than subpulmonary longitudinal strain (-12.8 $\pm$ 3.3% vs. -18.3 $\pm$ 3.8%; p $<$ 0.001). In contrast, LV global strain in subsystemic vs. subpulmonary position was similar: LV circumferential strain (-23 $\pm$ 13.1% vs. -20.2 $\pm$ 3.9%; n.s.); LV longitudinal strain (-17.5 $\pm$ 4.6% vs. -16.1 $\pm$ 5.3%; n.s.).
The subsystemic RV showed lower circumferential (-16.1 $\pm$ 2.9% vs. -23 $\pm$ 13.1%; p $<$ 0.05) and lower longitudinal strains (-12.8 $\pm$ 3.3% vs. -17.5 $\pm$ 4.6%; p $<$ 0.001) than the subsystemic LV. The subpulmonary LV exerted greater circumferential strains (-20.2 $\pm$ 3.9% vs. -13.1 $\pm$ 4.3%; p $<$ 0.001) but similar longitudinal strains compared to the subpulmonary RV (-16.1 $\pm$ 5.3% vs. -18.3 $\pm$ 3.8%; n.s.).
Conclusions: In discordant ventriculo-arterial connection, the subsystemic RV adapts to the increased afterload with an increase in circumferential strain and an impaired longitudinal deformation. This may represent the effect of a positive interventricular interaction

due to the shared circumferential fibers, since the LV shows higher circumferential strain than the RV even in subpulmonary position.

ORAL AB AGORA | **ORAL AB AGORA** | **ORAL AB AGORA** | Friday May 13| 16:10—16:55

1633

Three-dimensional vortex formation in patients with a Fontan circulation: evaluation with 4D flow CMR

Vivian P. Kamphuis[1,2]; Mohammed S.M. Elbaz[3]; Lucia J.M. Kroft[3]; Rob J. van der Geest[3]; Albert de Roos[3]; Nico A. Blom[1]; Jos J.M. Westenberg[3]; Arno A.W. Roest[1]
[1]Department of Pediatrics, division of Pediatric Cardiology, Leiden University Medical Center, Leiden, the Netherlands; [2]Netherlands Heart Institute, Utrecht, The Netherlands; [3]Department of Radiology, Leiden University Medical Center, Leiden, the Netherlands

Introduction: In the normal heart, formation of ring-shaped vortex flow has been suggested to help efficient blood flow during early (E) and late (A) diastolic filling of the left ventricle (LV), while altered vortex formation can be associated with LV abnormalities and inefficient blood flow [1,2,3]. Patients with a Fontan circulation have various underlying cardiac anatomy and it is unknown how this relates to vortex formation during diastolic filling. The purpose of this study was to assess three-dimensional (3D) vortex formation in patients with a Fontan circulation with different underlying pathologies, using four-dimensional (4D) flow CMR.
Methods: 11 patients with a Fontan circulation (age 15 $\pm$ 5 years) were evaluated by 4D flow CMR. Whole-heart 4D Flow CMR scans were performed on a 3 Tesla MRI (Ingenia, Philips Healthcare) with three-directional velocity-encoding of 150 cm/s in all directions, acquired voxel size of 3 $\times$ 2.6 $\times$ 3 mm3 and 30 phases reconstructed over one cardiac cycle. 3D vortex formation was identified in the LV at E- and A-diastolic filling, using the Lambda2 (λ2)-method [2]. Vortex formation during E- and A-diastolic filling was visually assessed.
Results: Vortex flow was present in all 11 patients at peak E-filling and in 10 patients at peak A-filling. One patient (with no A-wave) had no vortex during A-filling. Table 1 shows the versatile vortex formation in these patients. Normal "ring-shaped"' vortices were present in four patients. A double vortex ring ("eight-shaped") was present in four patients with two functional atrioventricular (AV)-valves (Figure 1a). One patient showed a large vortex ring along the ventricular septal defect (VSD) with protrusion in both ventricles (Figure 1b). Triangular vortices were present in two hypoplastic left heart syndrome (HLHS) patients (Figure 1c). Two patients showed a vortex ring with reversed septal-lateral orientation compared to other patients, which could be related to the asymmetric length of the AV-valve leaflets [3].
Conclusion: Altered 3D vortex formation is present in patients with a Fontan circulation during E- and A-filling and can be related to the different underlying pathologies. Future studies have to reveal the influence of this abnormal vortex formation on cardiac function.
References:
1. Kilner et al. Nature 2000
2. Elbaz et al. JCMR 2014
3. Calkoen et al. JTCVS 2015

Table 1 vortex formation during in Fontan patients with different underlying pathologies.

Patient	Underlying pathology	Vortex shape during early diastolic filling	Vortex shape during late diastolic filling
1	HLHS	Helix	Ring
2	DORV	large vortex ring with protrusion in both ventricles	double vortex ring
3	TGA	double vortex ring	double vortex ring
4	TA	Ring	Ring
5	HLHS	Ring	triangular
6	DILV	Helix	double vortex ring
7	HLHS	Ring	Ring
8	TGA	Reversed vortex ring	Reversed vortex ring
9	HLHS	triangular	triangular
10	TA	Reversed vortex ring	Reversed vortex ring
11	DILV	double vortex ring	No vortex

HLHS = hypoplastic left heart syndrome, DORV = double outlet right ventricle, TGA = transposition of the great arteries, TA = tricuspid atresia, DILV = double inlet left ventricle.

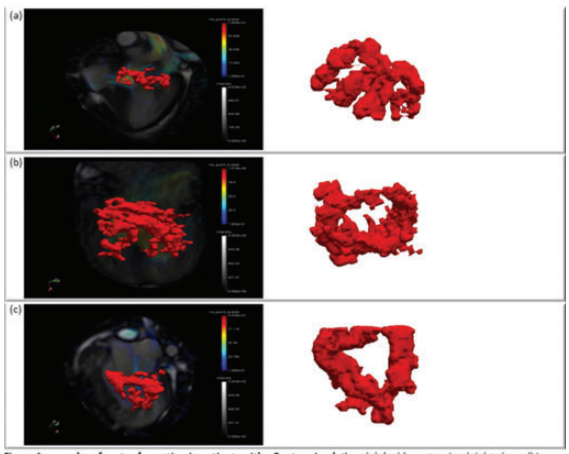

Figure 1 examples of vortex formation in patients with a Fontan circulation. (a) double vortex ring (eight-shaped) in a patient with double inlet left ventricle. (b) large vortex ring in a patient with double outlet right ventricle and a complete atrioventricular septal defect. (c) triangular shaped vortex in a patient with hypoplastic left heart syndrome.

ORAL AB AGORA | **ORAL AB AGORA** | **ORAL AB AGORA** | Friday May 13| 16:10—16:55

1483

Mitral valve prolapse: arrhythmogenic substrates by cardiac magnetic imaging

Manuel De Lazzari; Alberto Cipriani; Angela Susana; Stefania Rizzo; Benedetta Giorgi; Lacognata Carmelo; Emanuele Bertaglia; Barbara Bauce; Domenico Corrado; Gaetano Thiene; Martina Perazzolo Marra; Cristina Basso; Sabino Iliceto
Department of Cardiac, Thoracic and Vascular Sciences, University of Padova; Radiology, University of Padova, Italy

Introduction: Mitral valve prolapse (MVP) is a common valvular disorder with a benign prognosis in the vast majority of patients, but with an incidence of sudden cardiac death (SCD) twice than in the general population. Recent data support the theory that left ventricular (LV) fibrosis constitutes the substrate of SCD in MVP patients. Cardiac Magnetic Resonance (CMR) represents a noninvasive imaging modality that provides a comprehensive characterization of both the valve and the myocardium.
Aim: To assess the presence of myocardial substrates as scar in patients with MVP and arrhythmias.
Methods: We enrolled consecutive patients with MVP diagnosed by an 2D echocardiography. For each one we detect the presence of ventricular arrhythmias by a 24 hours 12-leads ECG continuous monitoring. All patients underwent complete CMR scan including post contrast sequences. Complex ventricular arrhythmias (LV-CVA) were defined as non sustained or sustained ventricular tachycardia exclusively with right bundle branch block (RBBB) morphology suggesting an origin from LV. Patients with moderate or severe mitral valve regurgitation or other cardiomyopathies were exclude.
Results: a total of 52 patients were enrolled (33 female, median age 44 years); a bileaflet MVP was found in 31 (60%). On the basis of presence of significant ventricular arrhythmias, a group of "arrhythmic MVP" (N:33) compared to "non-arrhythmic MVP" (N:19) patients were identified. No differences on ventricular volumes and function were found. On post-contrast sequences, LV LGE was identified in 36 (69%). The LGE location was at the level of papillary muscles in 28 patients (54%) and LV infero-basal segment, near posterior valve leaflet annulus, in 26 (50%). The presence of LV-LGE was associated with LV-CVA [32 (97%) vs 4 (21), $p < 0.001$].
Conclusions: arrhythmic MVP patients are characterized by a myocardial substrate of electrical instability detectable by CMR, such as LGE both of papillary muscle and infero-basal LV wall. This points may represent area stretched by abnormal valve excursion leading to a local fibrosis, as confirmed also by post mortem analysis. The management of MVP patients with LGE by CMR, whether drugs, catheter ablation or ICD, remains a clinical challenge requiring further studies.

ORAL AB AGORA | **ORAL AB AGORA** | **ORAL AB AGORA** | Friday May 13| 16:10—16:55

1596

Increased local wall shear stress after coarctation repair is associated with descending aorta pulse wave velocity: evaluation with CMR and 4D flow

I. Nederend; A.A.W. Roest; P.J. van den Boogaard; A.D.J. ten Harkel; J.C.N. de Geus; L.J.M. Kroft; A. de Roos; J.J.M. Westenberg
VU Amsterdam, Leiden University Medical Center, The Netherlands

Background: Coarctation of the aorta (CoA) is a local narrowing of the descending aorta (AO), typically distal from the left subclavian artery. Curative operational treatment is available and survival in childhood is good. However, in adulthood complications including hypertension, restenosis and aneurysm formation are not uncommon. In this explorative CMR study, we sought to investigate whether an association exists between AO wall compliance (expressed in pulse wave velocity (PWV) and distensibility) and 3D wall shear stress (WSS) in the AO in children after CoA repair.
Methods: 19 patients aged 12.8 $\pm$ 3 years underwent 4D flow CMR on 3T MRI (Ingenia, Philips Healthcare). 14 patients had a bicuspid aortic valve and none of the patients had clinical indication for re-intervention. 19 healthy volunteers aged 13.2 $\pm$ 3 years were included to assess normal values of PWV. PWV was determined from high-temporal 1-directional velocity encoding, for both proximal AO (ascending AO plus aortic arch) as well as the descending AO. Distensibility was measured at the ascending AO from the lumen area distension and the brachial pulse pressure. 3D WSS was determined from 4D flow CMR using CAAS MR 4Dflow v1.0 software (Pie Medical Imaging).
Results: There was no difference in age between volunteers and patients ($p = 0.901$). Proximal AO PWV (4.3 $\pm$ 0.9 m/s; in controls vs 5.0 $\pm$ 1.4 m/s in patients) and descending AO PWV (4.1 $\pm$ 0.9 m/s vs 3.9 $\pm$ 0.9 m/s) were not significantly different between both groups ($p = 0.499$ and $p = 0.538$ respectively). Ascending AO distensibility and proximal AO PWV were correlated ($r = -.62$; $p = 0.008$) in patients as expected, but not in volunteers due to the narrow range in both parameters. No relationship was found between overall WSS and PWV ($r = -.053$ $p = 0.846$) in entire AO but peak WSS in the aortic arch and proximal AO PWV were correlated ($r = -.550$ $p = 0.027$). The average ratio of peak WSS near the repaired CoA to average WSS in the entire AO was 2.6 $\pm$ 0.5 and this ratio was correlated to descending AO PWV ($r = .518$; $p = 0.04$).
Conclusion: Regional AO wall compliance measured by PWV was not significantly different between young controls and patients after CoA repair. However, at the repaired site, local WSS is more than doubled in patients, and this is associated with PWV distal to the CoA site. The AO seems to be locally affected in the distal rather than proximal AO.

Altered wall compliance and WSS may in part explain the long term sequela in patients after CoA repair.

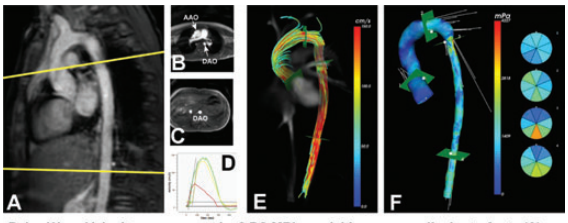

Pulse Wave Velocity assessment by 2 PC MRI acquisitions perpendicular to Aorta (A), resulting in flow velocity-time curves (D) at Ascending Aorta (AAO) (B), proximal and distal Descending Aorta (DAO) (B+C). E represents streamline visualization of 4D flow of aorta in a patient with repaired coarctation. F represents 3D wall shear stress.

ORAL AB AGORA | **ORAL AB AGORA** | **ORAL AB AGORA** | Friday May 13| 16:10—16:55

1636

Three-dimensional wall shear stress assessed by 4Dflow CMR in bicuspid aortic valve disease

Lydia Dux-Santoy[1]; Raquel Kale[1]; Gisela Teixido-Tura[1]; Giuliana Maldonado[1]; Marina Huguet[2]; David Garcia-Dorado[1]; Artur Evangelista[1]; Jose Rodriguez-Palomares[1]
[1]Hospital Vall d'Hebron, Universitat Autònoma de Barcelona, Barcelona, Spain; [2]CETIR-Pilar-Sant Jordi Clinic, Barcelona, Spain

Background: Ascending aorta (AAo) aneurysms may be partially caused by altered flow patterns associated with bicuspid aortic valve (BAV). Wall shear stress (WSS) has been hypothesized as an important biomarker for aortic dilatation. Thus, specific WSS patterns could potentially explain the development of a certain phenotype in BAV patients. The aim of our study was to analyze differences in WSS patterns using 3D maps according to the BAV morphotype.
Methods: Eighty-six BAV patients with no severe valvular disease and aortic diameters under 50 mm were enrolled. Fusion phenotype was right-left (RL-BAV) in 65 patients, and right-non coronary (RN-BAV) in 21. All subjects underwent 4D Flow MRI with retrospective cardiac gating at 1.5 T. Eight double-oblique analysis planes were equally distributed in the AAo between the sinotubular junction and the origin of the brachiocephalic trunk. Peak-systolic WSS was calculated in each plane, as described by Stalder et al. 3D WSS maps were estimated by longitudinally interpolating these WSS values. Peak velocity, flow eccentricity and rotational flow were evaluated in three slices located at proximal (S2), mid (S4) and distal AAo (S8). Calculations were performed using custom Matlab software.
Results: Table 1 summarizes differences between RL-BAV and RN-BAV in peak velocity, eccentricity and rotational flow at different aortic levels. RN-BAV had higher peak velocities and rotational flow. Different BAV phenotypes presented different outflow jet direction that correlated with the distribution of WSS within the aortic wall. Thus, RN-BAV patients presented a maximum WSS from proximal left posterior-to-distal right aortic wall (figure 1b) while the maximum WSS was from left posterior-to-right anterior at proximal-medial levels in RL-BAV patients (figure 1a).

		Peak velocity (cm/s)	Jet Angle (°)	Normalized Displacement	Rotational Flow (cm²/s)
S2	RL-BAV	127.8 ± 27.1	22.2 ± 10.8	0.152 ± 0.068	124.0 ± 109.9
	RN-BAV	146.4 ± 24.3	26.4 ± 11.3	0.135 ± 0.077	212.2 ± 125.3
S4	RL-BAV	118.5 ± 28.2	22.4 ± 11.8	0.109 ± 0.073	183.0 ± 149.5
	RN-BAV	124.5 ± 28.1	28.5 ± 12.1	0.112 ± 0.061	241.3 ± 197.0
S8	RL-BAV	104.3 ± 28.0	25.6 ± 9.1	0.052 ± 0.034	85.9 ± 95.8
	RN-BAV	109.0 ± 29.9	22.4 ± 9.2	0.059 ± 0.034	191.1 ± 170.7

Table 1. Mean ± SD values at three locations (S2, S4, S8) for RL and RN fusion patterns of BAV

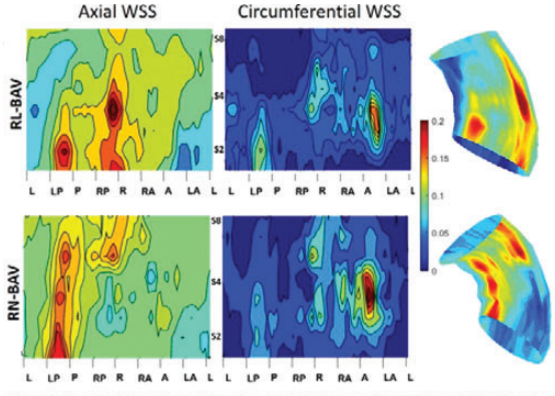

Figure 1. Axial and circumferential peak-systolic WSS maps of typical RL and RN BAV patients

Conclusion: Maximum AAo-WSS region varies according to the BAV morphotype. 3D WSS maps can precisely illustrate these surface variations in WSS and can be a useful tool to better understand the pathophysiology of aortic dilatation in these patients.

ORAL AB AGORA | **ORAL AB AGORA** | **ORAL AB AGORA** | Saturday May 14| 10:25—11:10

1464

Cardiac Amyloidosis and Aortic Stenosis – The Convergence of Two Aging Processes

João L. Cavalcante; Shasank Rijal; John T. Schindler; Thomas G. Gleason; Joon S. Lee; Erik B. Schelbert
University of Pittsburgh School of Medicine/UPMC

Background: Senile cardiac amyloidosis (SCA), once thought to be a rare disease, has been commonly diagnosed with Cardiac MRI (CMR). Recent autopsy series in octogenarians with severe aortic stenosis who received transcatheter aortic valve replacement reported prevalence up to 30%.
Objectives: To evaluate the prevalence of SCA detected by CMR in patients with confirmed moderately-severe symptomatic aortic stenosis (AS) and its association with clinical outcomes.
Methods: 95 consecutive AS patients (85% with severe AS) who underwent CMR study (1.5T Siemens Magnetom Espree) and echocardiogram within 15 days (median 6 days, IQR 0-15) were included in the analysis. Society of Thoracic Surgery predicted risk of mortality (STS-PROM) was calculated for each patient using over 40 clinical parameters. SCA was identified when characteristic pattern involving either subendocardial or diffuse myocardial LGE was observed. Cox-proportional hazards model performed after adjusting for potential confounders to evaluate the independent prognostic role of AS + SCA.
Results: A total of 9 patients (8 males, 89%) had AS + SCA (10% prevalence). Clinical, imaging and outcomes are listed in Table 1. Patients with AS + SCA were older than those with only AS (87 ± 5 vs. 68 ± 5 years, $p < 0.0001$) and had higher STS-PROM (6.8 ± 4.2 vs. 3.3 ± 3.2 %, $p = 0.003$). Over median follow-up of 10 months (IQR: 3- 19 months), there were 28 deaths (30%) and 39 AVRs (31 surgical and 8 transcatheter). There was no difference in the percentage of AVR performed in AS + SCA vs. isolated AS (33% vs. 42%, $p = 0.73$). Despite adjustment for AVR (HR = 0.51, 95% CI 0.22-1.18, $p = 0.11$) and STS-PROM (HR = 1.16, 95% CI 1.07-1.25, $p < 0.0001$), presence of AS + SCA was an independent predictor of all-cause mortality (HR = 4.02, 95% CI = 1.3-12.7, $p = 0.02$).
Conclusion: SCA is not uncommon in octogenarians presenting with symptomatic severe AS. One year all-cause mortality in AS + SCA patients was 3 times higher than in patients with isolated severe AS (Figure 1). Whether this risk can be modulated by additional therapies, beyond AVR, requires future studies.

Table 1. Clinical, Imaging Characteristics and Outcomes of Patients with AS + SCA

	Patient 1	Patient 2	Patient 3	Patient 4	Patient 5	Patient 6	Patient 7	Patient 8	Patient 9
Age/Gender	82/M	98/M	89/F	85/M	87/M	81/M	88/M	86/M	95/M
EKG Rhythm	Afib	Afib	Afib	Afib	NSR	NSR	S. Tach	Afib	Afib
Low Voltage Criteria	No	No	No	No	No	No	No	No	No
ECHOCARDIOGRAPHIC FINDINGS									
IV septum/Post Wall Thick (cm)	2.0/1.9	1.7/1.5	1.7/1.4	1.9/1.5	1.8/1.5	1.9/1.5	1.6/1.6	2.1/1.9	1.6/1.6
Aortic Valve Area (cm²)	0.3	0.7	0.4	0.9	0.6	0.8	0.6	1.1	0.5
Mean AV Gradient (mmHg)	18	33	33	13	30	47	37	12	50
CMR FINDINGS									
LVEF (%)	23	45	35	53	35	67	18	49	51
LV End-Diast Vol Index (ml/m²)	104	64	93	60	94	47	91	88	101
LV Mass Index (g/m²)	101	103	97	113	108	73	84	139	128
OUTCOMES									
Aortic Valve Replacement	No	No	TAVR	No	TAVR	No	No	No	TAVR
Status	Dead	Dead	Dead	Alive	Alive	Alive	Dead	Alive	Dead
Survival after CMR (months)	1	2	3	6	8	8	3	5	2

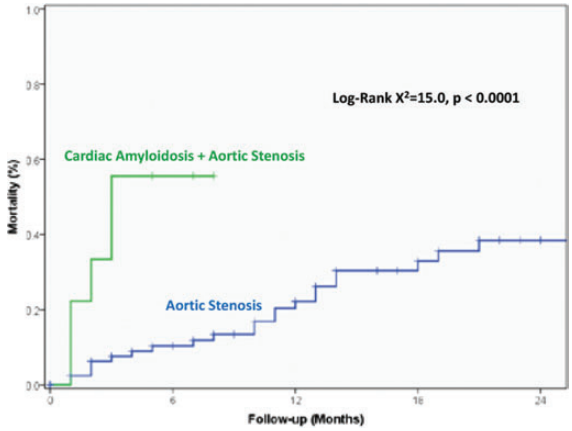

Figure 1. Kaplan-Meier Curves Comparing All-Cause Mortality in AS vs. AS + SCA Patients

ORAL AB AGORA | **ORAL AB AGORA** | **ORAL AB AGORA** | Saturday May 14| 10:25—11:10

1630

Blood T1 variability explained in healthy volunteers: an analysis on MOLLI, ShMOLLI and SASHA

Stefania Rosmini[1]; Heerajnarain Bulluck[1]; Thomas A Treibel[1]; Anish Bhuva[1]; Amna Abdel-Gadir[1]; Veronica Culotta[1]; Ahmed Merghani[2]; Viviana Maestrini[1]; Anna S Herrey[1]; Peter Kellman[2]; Charlotte Manisty[1]; James C Moon[3]
[1]Barts Heart Centre, St Bartholomew's Hospital, London, UK; [2]Department of Cardiovascular Sciences, St Georges, University of London, London, United Kingdom; [3]National Heart, Lung and Blood Institute, National Institutes of Health, Bethesda, USA

Background: Native myocardial T1 is known to be affected by variables such as age, gender, heart rate and partial voluming from blood pool. Blood T1 itself has a wider variability. We aimed to investigate causes of blood T1 variability.
Methods: 77 healthy volunteers with no known cardiovascular condition underwent CMR at 1.5T (Siemens, Avanto). Mid ventricular short axis native T1 maps by MOLLI (with T1* reconstruction in addition), ShMOLLI and SASHA were acquired. Hematocrit (Hct), iron profile and lipid profile were acquired immediately prior to the scan. CVI42 (Calgary, Canada) was used for analysis of the maps. A ROI was drawn in the blood pool on the MOLLI T1 map, avoiding papillary muscles, and was copied onto the MOLLI T1*, ShMOLLI and SASHA T1 maps.
Results: Complete datasets of blood and maps were available for all 77 volunteers (mean age 49 $\pm$ 14, range 20-76, 49% males). Mean $\pm$ SD of blood T1 by MOLLI T1 was 1638 $\pm$ 78ms, MOLLI T1* 1686 $\pm$ 111ms, ShMOLLI T1 1543 $\pm$ 77ms and SASHA 1584 $\pm$ 100ms. There was a negative correlation between blood T1 and Hct (R2 0.530, coeff. -0.728, $p <$ 0.0001). Hct, iron, HDL-cholesterol, ferritin, triglicerides (TG), LDL-cholesterol and total iron binding capacity (TIBC) resulted to be significant at univariate analysis while this was not the case for albumin and total cholesterol. The multivariate analysis performed including only the significant variables showed that Hct, iron and HDL-cholesterol are significantly correlated with blood T1 by MOLLI T1 and T1*, ShMOLLI and SASHA (Table 1).
Conclusions: In health, Hct, iron and HDL-cholesterol explain almost all (90%) of blood T1 variability with anaemia and low iron increasing T1 but with HDL reducing it.

Table 1. Univariate and multivariate analysis for blood variables and blood T1 by MOLLI T1, MOLLI T1*, ShMOLLI and SASHA.

	MOLLI Blood T1			MOLLI Blood T1*			ShMOLLI Blood T1			SASHA Blood T1		
Univariate	R	slope	p	R	slope	p	R	slope	p	R	slope	p
HCT	-0.672	-1458	<0.0001	-0.707	-2184	<0.0001	-0.728	-1556	<0.0001	-0.612	-1743	<0.0001
Iron	-0.694	-326	<0.0001	-0.583	-390	<0.0001	-0.636	-295	<0.0001	-0.431	-266	<0.0001
HDL-chol	0.452	248	<0.0001	0.427	334	<0.0001	0.478	260	<0.0001	0.570	411	<0.0001
Ferritin	-0.309	-61	0.006	-0.367	-103	0.001	-0.336	-65	0.003	-0.278	-2.6	0.007
TG	-0.321	-109.1	0.004	-0.251	-121.5	0.028	-0.331	-110.7	0.003	-0.395	-176	<0.0001
LDL-chol	-0.217	-143.1	0.059	-0.122	-114.8	0.291	-0.208	-135.6	0.069	-0.270	-235	0.009
TIBC	0.152	191.2	0.188	0.273	490.1	0.016	0.188	233.8	0.102	0.111	185	0.167
Albumin	0.042	1.2	0.717	-0.009	-0.36	0.94	0.023	0.651	0.844	-0.002	-0.081	0.493
Total chol	0.021	1.8	0.857	0.111	13.5	0.335	0.043	3.6	0.713	0.018	1.96	0.440
Multivariate	Cum R2	slope	p	Cum R2	slope	p	Cum R2	slope	p	Cum R2	slope	p
Hct		-936.5	<0.0001		-1603.5	<0.0001		-1085.5	<0.0001	0.764	-1114	<0.0001
Iron		-255.1	<0.0001		-275.5	<0.0001		-213.9	<0.0001		-168	<0.0001
HDL-chol	0.88	129.5	<0.0001	0.831	152.2	0.007	0.884	132.1	<0.0001		288	<0.0001

ORAL AB AGORA | **ORAL AB AGORA** | **ORAL AB AGORA** | Saturday May 14| 10:25—11:10

1408

Myocardial deformation on CMR predicts adverse outcomes in carcinoid heart disease - a new marker of risk

B. Liu[1]; M.K. Hayer[1]; S. Baig[1]; T. Shah[2]; S.J. Rooney[3]; N.C. Edwards[1]; R.P. Steeds[1]
[1]Department of Cardiology; [2]Hepatology & Cardiovascular Surgery; [3]Queen Elizabeth Hospital Birmingham & Institute of Cardiovascular Science, University of Birmingham

Introduction: Carcinoid heart disease (CHD) is a frequent and adverse complication of carcinoid syndrome due to right ventricular (RV) failure. Medical therapy has a 2-year survival of 20% and while surgical valve replacement is effective in improving symptoms and may increase survival, peri-operative risk remains 15-20%. Echocardiography is considered gold standard for assessing CHD and data on the role of cardiacmagnetic resonance imaging (CMR) are limited despite recognised advantages in assessment of theright heart. This study aims to assess the role of CMR in the assessment of CHD.
Methods: 50 consecutive patients with proven neuroendocrine tumours were referred with elevated NT pro-BNP to the European Centre of Excellence for Neuroendocrine Tumours in Birmingham between 2005-2015. At referral, all subjects underwent comprehensive left ventricular (LV) and RV assessment with CMR (1.5T Siemens Avanto), including deformation (Tissue Tracking, Circle cvi42), and late gadolinium enhancement (LGE).
Results: 36 patients were diagnosed with CHD and 14 without (CHD-neg). RV valve disease was universal in CHD: severe tricupid regurgitation (97%), severe pulmonary regurgitation (86%). On CMR, RV end-diastolic volume (EDV) and end-systolic volume (ESV) were increased (120 $\pm$ 30 vs. 67 $\pm$ 14 ml/m2, $p <$ 0.01; 49 $\pm$ 20 vs. 11 $\pm$ 3ml/m2, $p <$ 0.01) but with no difference in RVEF (60 $\pm$ 14% vs. 60 $\pm$ 9% $p =$ 0.92). There was early evidence of ventricular-ventricular interaction, with reduction in LVEDV (53 $\pm$ 16 vs. 72 $\pm$ 16 ml/m2, $p <$ 0.01) and LVESV (19 $\pm$ 10 vs. 28 $\pm$ 16ml/m2, $p <$ 0.05) in CHD but no difference in LVEF (67 $\pm$ 8% vs. 63 $\pm$ 14%, $p =$ 0.3). There was no difference in LV global longitudinal strain (GLS) or circumferential strain (GCS) between groups. RV LGE indicative of endocardial plaques was present in 6/36 (17%) but not observed in CHD-neg. Diffuse LV LGE was present 5 CHD patients. Over follow up (median 1.3 years [0.6-3.1]), 20 patients with CHD died. These patients had a lower GCS (14.8 $\pm$ 4.6% vs. 18.2 $\pm$ 4.4%, $p <$ 0.05) and lower GLS (14.7 $\pm$ 4.7% vs. 18.3 $\pm$ 4.4%, $p <$ 0.05) on CMR but no difference in ventricular size, EF or NT-proBNP. In a logistic regression model, LV GLS remained an independent predictor of death.
Conclusion: Significant increase in RV size and the presence of RV plaques are measurable on CMR early following referral with CHD. This is sufficient to adversely affect LV filling and global deformation, which may contribute to effort intolerance and adverse outcomes.

ORAL AB AGORA | **ORAL AB AGORA** | **ORAL AB AGORA** | Saturday May 14| 10:25—11:10

1492

Myocardial Perfusion Reserve and Global Longitudinal Strain in Early Rheumatoid Arthritis

G.J. Fent; P. Garg; P. Swoboda; L.E. Dobson; T.A. Musa; J.F. Foley; P. Haaf; J.P. Greenwood; S. Plein
LICAMM, University of Leeds, United Kingdom

Objectives: Rheumatoid arthritis (RA) is a systemic inflammatory condition associated with increased cardiovascular mortality compared with the general population. Proposed mechanisms for this increased mortality include coronary microvascular dysfunction due to immune dysregulation and systemic inflammation.
First pass myocardial perfusion CMR allows quantification of myocardial blood flow (MBF) from which myocardial perfusion reserve (MPR) can be derived. In the absence of epicardial coronary artery disease, reduced MPR represents coronary microvascular dysfunction. We therefore hypothesised MPR would be reduced in RA patients.
Additionally, we hypothesised that abnormalities in left ventricular (LV) deformation would be evident in RA patients, as LV mass has been reported to be reduced in established disease.
Methods: Twelve patients with newly diagnosed, treatment naïve RA and 12 healthy volunteers (HV) underwent CMR at 3.0T (Phillips Achieva TX). Both groups had no history of coronary artery disease or additional risk factors for this. Dual bolus resting and stress perfusion imaging was performed (0.1mmol/kg Gadolinium DTPA) and MBF values for the mid ventricular slice were estimated using Fermi constrained convolution (PMI v 0.4 [Sourbron, 2009]). MPR was calculated by dividing stress MBF by rest MBF. Left ventricular ejection fraction (LVEF) and global longitudinal strain (GLS) by feature tracking were calculated using bSSFP images (CVI 42, Circle Cardiovascular Imaging, Calgary, Canada).
Results: Mean age of RA patients was 48 $\pm$ 16 and mean age of HV 47 $\pm$ 14. Of the RA patients, were 4 were male and 8 were female. Of the HV, 2 were male and 10 were female. Mean values for MPR were 1.98 $\pm$ 0.79 and 1.99 $\pm$ 0.72 ($P =$ 0.88) for RA and HV respectively. Mean values for LVEF were 63 $\pm$ 4 and 62 $\pm$ 4% ($P =$ 0.48) respectively for RA patients and HV. Mean values for GLS were -20.2 and -21 $\pm$ 0.4 ($P =$ 0.396) for RA and HV respectively.
Conclusion: These preliminary findings from the CADERA trial suggest that, newly diagnosed, treatment naïve RA patients have no detectable abnormalities on perfusion CMR compared with HV. Therefore, whilst present in established RA, coronary microvascular dysfunction may not yet have developed in early RA. Additionally, no abnormalities of LV systolic function were evident in newly diagnosed RA and may be a later manifestation of the disease.

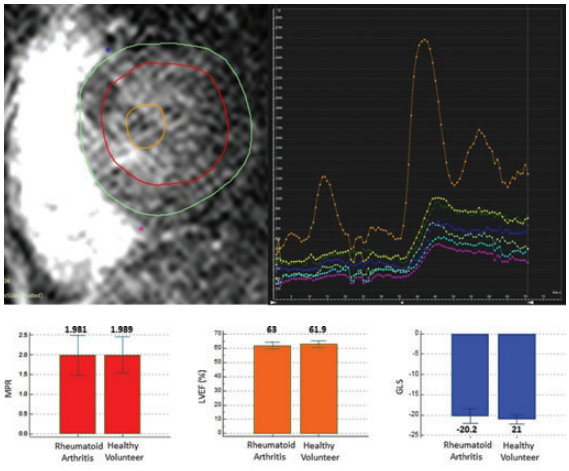

ORAL AB AGORA | **ORAL AB AGORA** | **ORAL AB AGORA** | Saturday May 14| 10:25—11:10

1500

Exercise CMR to differentiate athlete's heart from patients with early dilated cardiomyopathy

G. Claessen; F. Schnell; J. Bogaert; S. Dymarkowski; N. Pattyn; P. Claus; J. Van Cleemput; A. La Gerche; H. Heidbuchel
Department of Cardiovascular Medicine and Department of Imaging & Pathology, KU Leuven, Belgium; University of Hasselt and Heart Center, Jessa Hospital, Hasselt, Belgium

Introduction: It can be difficult to distinguish between early stage dilated cardiomyopathy (DCM) and left ventricular (LV) dilation with mildly reduced LV ejection fraction (EF) which is a relatively common observation amongst endurance athletes (EAs). This has important consequences for clearance for competitive sport participation since DCM may precipitate fatal ventricular arrhythmias.
Methods: We prospectively included 9 EAs and 9 asymptomatic patients with mild DCM (7 familial DCM and 2 partially recovered severe DCM), all LVEF 40-55% at inclusion. In all subjects beta-blockers were withheld 24 hours before evaluation. First, cardiopulmonary exercise testing was performed to determine maximal power (Pmax). Then, cardiac magnetic resonance (CMR) imaging was performed at rest and during bicycle exercise at 25%, 50% and 66% of Pmax to determine left and right ventricular (RV) end-diastolic and end-systolic volumes, from which ejection fraction (EF) was calculated.
Results: At rest, RVEF was lower in EAs than in DCM patients, whereas LVEF was similar (Figure 1A). At peak exercise, RVEF was similar in both groups. However, LVEF augmentation was observed in EAs but was attenuated in DCM patients. Receiver-operator characteristic curves demonstrated that a cut-off value of 11.2% for the increase in LVEF from rest to peak exercise (ΔLVEF) had a sensitivity of 89% and specificity of 89% to differentiate EAs from DCM patients [AUC = 0.89(0.72-1.06); P = 0.005], whereas resting LVEF (cut-off: 50.8%) was not predictive (Figure 1B).
Conclusion: Evaluation during exercise facilitates the differentiation between athlete's heart and DCM. An athlete's heart demonstrates good myocardial contractile reserve as compared to subjects with early DCM in whom LV functional reserve is reduced.

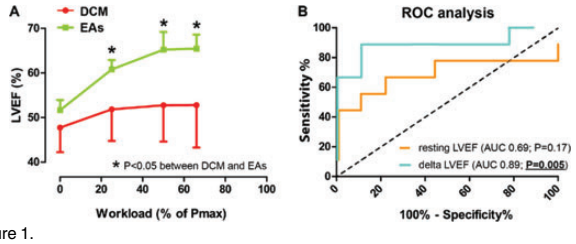

Figure 1.

ORAL AB AGORA | **ORAL AB AGORA** | **ORAL AB AGORA** | Saturday May 14| 10:25—11:10

1559

Real-Time, x-mri guidance to optimise left ventricular lead placement for delivery of cardiac resynchronisation therapy

Jonathan Behar; Daniel Toth; Sabrina Reiml; Maria Panayiotou; Simon Claridge; Tom Jackson; Manav Sohal; Jessica Webb; Mark O'Neill; Alexander Brost; Peter Mountney; Reza Razavi; Kawal Rhode; Christopher Aldo Rinaldi
St Thomas' Hospital, London, UK

Suboptimal LV lead placement contributes to cardiac resynchronization therapy (CRT) non-response. Cardiac MR (CMR) identifying myocardial scar & dyssynchrony allows targeted LV lead placement. Currently CMR is performed prior & separate to implantation. We describe a novel guidance platform, integrated within an XMR facility enabling CMR data acquisition, processing & analysis with immediate overlay onto live fluoroscopy.
Methods and Results: Short & long axis cines & late gadolinium sequences are segmented and projected onto a 16-segment AHA model demonstrating location, transmurality & burden of myocardial fibrosis. Regional motion analysis demonstrates the latest mechanical activating segments. This process is performed seamlessly while the patient is within the XMR suite allowing segmented LV geometry/scar to be immediately co-registered with fluoroscopy. CS venography is overlaid onto the 3D-shell to identify the preferential targets for LV stimulation. This platform has been successfully used in 6 patients with no significant increase in procedure time or radiation dose compared with our historical controls (89 ± 18 vs.113 ± 28 minutes & 826 ± 191 vs. 950 ± 450 cGycm2, p = ns). Late, target segments avoiding scar were paced in all cases. Visualization of the target informed positioning of the LV lead and enabled identification of the optimal poles to use for biventricular stimulation (Figure).
Conclusion: Performing and processing CMR data in real time is feasible and may aid optimal LV lead placement for CRT delivery. This can be accomplished in a single sitting with no delay between CMR and CRT implant.

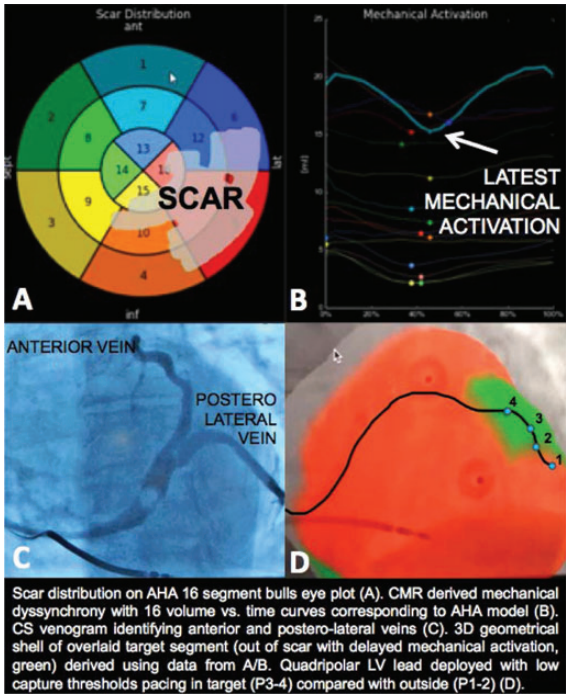

Scar distribution on AHA 16 segment bulls eye plot (A). CMR derived mechanical dyssynchrony with 16 volume vs. time curves corresponding to AHA model (B). CS venogram identifying anterior and postero-lateral veins (C). 3D geometrical shell of overlaid target segment (out of scar with delayed mechanical activation, green) derived using data from A/B. Quadripolar LV lead deployed with low capture thresholds pacing in target (P3-4) compared with outside (P1-2) (D).

ORAL AB AGORA | **ORAL AB AGORA** | **ORAL AB AGORA** | Saturday May 14| 10:25—11:10

1560

The role of Cardiac magnetic resonance imaging in patients undergoing ablation for ventricular tachycardia- Defining the substrate and visualizing the outcome

S. Oebel; A. Arya; S. Hilbert; A. Bollmann; G. Hindricks; C. Jahnke; I. Paetsch; B. Dinov
Heart Center Leipzig, Leipzig, Germany

Background: Pre- interventional Cardiac Magnetic Resonance (CMR) imaging may help to identify the underlying arrhythmogenic substrate in patients undergoing radiofrequency (RF) ablation for ventricular tachycardia (VT). However, the extent and characteristics of structural damage induced by the ablation itself and its association with acute procedural outcome remain poorly defined so far.
Methods: 17 patients (82% male, median age 57.5 ± 11 years, 6 with known coronary artery disease) who underwent VT ablation received CMR scans pre- and post- ablation. CMR was performed at 1.5 Tesla including cine, T2-weighted, 3D- early and late-gadolinium- enhancement (LGE)- imaging in standard cardiac geometries. LGE and microvascular obstruction (MO) were expressed as percentage of total left ventricular mass. The electrophysiological (EP) procedures were performed according to local protocols using the Carto©- Mapping- system in all cases. Non- inducibility of VTs at the end of the procedure was defined as the primary endpoint. RF ablation was performed using a 3.5 mm Thermocool catheter, flow rate 30 ml/min.
Results: In 13 patients, substrate defined as positive LGE, could be described on pre-interventional CMR imaging (11 endocardial, 1 endo- and epicardial, 1 strictly epicardial; mean LGE 22.6% ± 16). Mean left ventricular ejection fraction (LV-EF) before ablation was 45% ± 11. Successful ablation was performed in all cases using a mean maximum energy of 55 ± 11 Watt. Epicardial access was used in 3 patients.
On postinterventional scans, myocardial edema was visible in 9 patients. MO was present in all patients (mean MO 6 ± 2%, 7 cases with a MO >5%) Mean postinterventional LV-EF showed to significant difference to baseline (42%15, p = 0.4) and decreased in only 1 patient (MO> 5%). The extent of MO correlated significantly with the applied maximum energy (R = 0.625, p = 0.007) and the mean ablation time (R = 0.512, p = 0.036). A 100% transmural ablation lesion was observable in 4 patients.
Conclusion: Apart from reliably defining the arrhythmogenic substrate preinterventionally in patients with VTs undergoing ablation, postprocedural CMR imaging reveals acute myocardial injury in the form of edema and MO induced by the ablation itself. The extent of the lesions directly correlates with the time and the maximum power of the applied RF energy. Whether the lesion characteristics on are associated with short- and long- term outcome needs to be further assessed.

ORAL AB AGORA | **ORAL AB AGORA** | **ORAL AB AGORA** | Saturday May 14| 10:25—11:10

1590

Impact of cardiovascular magnetic resonance on clinical management and decision-making of out of hospital cardiac arrest survivors with inconclusive coronary angiogram

A. Baritussio[1,2]; M. Perazzolo Marra[2]; A. Ghosh Dastidar[1]; J. Rodrigues[1]; A. Zorzi[2]; A. Susana[2]; A. Scatteia[1]; E. De Garate[1]; G. Mattesi[2]; J. Strange[1]; D. Corrado[2]; C. Bucciarelli-Ducci[1]

[1]Bristol Heart Institute, Bristol NIHR Cardiovascular Biomedical Research Unit (BRU), Bristol, United Kingdom; [2]Department of Cardiac, Thoracic and Vascular Sciences, University of Padua, Padua, Italy

Background: Non-traumatic out of hospital cardiac arrest (OHCA) is the leading cause of death worldwide. Urgent coronary angiography is a class IB recommendation, as 2/3 of cases are secondary to acute coronary syndrome. However diagnosis and management of patients with unobstructed coronaries or unidentified culprit lesion on angiogram is challenging. We sought to assess the additive role of cardiac magnetic resonance (CMR) in patients with an inconclusive coronary angiogram and to determine the best CMR parameter in predicting clinical impact.

Methods: We analysed the CMR registry data of consecutive patients surviving non-traumatic OHCA, undergoing urgent angiogram and CMR from two tertiary cardiology centres. The study focused on the analysis of patients with an inconclusive angiogram, defined as unobstructed coronaries or coronary artery disease (CAD) without a clear culprit lesion. Clinical impact of CMR was defined as a change in diagnosis, as compared to a multi- parametric pre-CMR diagnosis, or a change in management, which could be a change in medication or the performance/avoidance of invasive procedures.

Results: Out of 174 OHCA survivors referred for CMR following urgent angiogram, we identified 110 patients (63%,84 male,mean age55 $\pm$ 17) with inconclusive angiogram: 73 patients(66%) had unobstructed coronaries and 37(34%) had CAD with no clear culprit. Diagnosis based on CMR findings was ischemic heart disease in 43 patients (39%), non-ischemic heart disease in 33 (30%), a structurally normal heart was found in 24 (22%) and non-specific findings in 10 (9%). Overall, CMR had a clinical impact in 72% of patients, determining a change in diagnosis in 25% of patients, a change in management in 30%, and a change in both in 17%. CMR led to revascularization in 20% of patients and to ICD implantation in 10%; an invasive procedure was avoided in 12% of patients. In a multivariate model including clinical and imaging parameters, the strongest predictors of the clinical impact of CMR were regional wall motion abnormality and the analysis of LGE sequences (p 0.042,95% CI 1.05-9.99; $p < 0.0001$,95% CI 5.46-73.7,respectively).

Conclusions: CMR had a clinical impact in more then two thirds of OHCA survivors with an inconclusive coronary angiogram. The analysis of LGE sequences was the strongest independent predictor of clinical impact following CMR. Given its additional role CMR should be incorporated in the clinical-diagnostic work-up of this group of patients.

ORAL AB AGORA | **ORAL AB AGORA** | **ORAL AB AGORA** | Saturday May 14| 10:25—11:10

1561

Detection of coronary stenosis at rest using Oxygenation-Sensitive Magnetic Resonance Imaging

J. Ranjit Arnold; Michael Jerosch-Herold; Theodoros D. Karamitsos; Jane M. Francis; Paul Bhamra-Ariza; Rizwan Sarwar; Robin Choudhury; Joseph B. Selvanayagam; Stefan Neubauer

University of Oxford Centre for Clinical Magnetic Resonance Research, John Radcliffe Hospital, Oxford, UK; Brigham & Women's Hospital & Harvard Medical School,Boston, USA; Department of Cardiovascular Medicine, Flinders Medical Centre, Adelaide, Australia

Objective: To determine whether Oxygenation-Sensitive Magnetic Resonance Imaging (MRI) can identify functionally significant coronary artery disease (CAD) without the need for stress.

Background: In the setting of CAD, microvascular dilation has been shown to occur in post-stenotic myocardium at rest. Microvascular volume is a determinant of signal intensity with Oxygenation-Sensitive (O-S) MRI. Therefore, we postulated that O-S imaging at rest could detect microvascular heterogeneity, and thereby identify coronary stenosis without recourse to physiological or pharmacological stress.

Methods: Rest O-S images were acquired at 3 Tesla using a T2-prepared ECG-gated steady-state free precession sequence and assessed quantitatively using a resting O-S index (interquartile range of segmental O-S signal intensities/median segmental signal intensity). First-pass perfusion images were also acquired at rest and stress (intravenous adenosine, 140 μg/kg/min) and assessed quantitatively using model-independent deconvolution. A threshold resting O-S index to identify myocardial ischaemia at the patient level (as defined quantitatively as $\geq$1 myocardial segment with hyperaemic myocardial blood flow $\leq$1.6ml/min/g) was first determined in a derivation arm comprising 25 patients with known CAD and 20 healthy volunteers. To determine diagnostic performance, this threshold was then applied in a separate validation group comprising 57 patients with suspected CAD referred for diagnostic angiography.

Results: Receiver-operating characteristic curve analysis defined a threshold resting O-S index of 16.1% to identify patients with myocardial ischaemia (72% sensitivity and 78% specificity; area under the curve 0.72 $\pm$ 0.08, $p = 0.0078$). Application of this threshold in the validation arm of the study yielded sensitivity 88%, specificity 58% and diagnostic accuracy 75% for the identification of subjects with ischaemia, and 82%, 61%, and 75%, respectively, for identifying those with significant coronary stenosis. At the patient level, there was reasonable agreement between resting O-S imaging and both first-pass perfusion (kappa $= 0.51$) and quantitative coronary angiography (kappa $= 0.48$).

Conclusions: O-S imaging indicates the presence of microvascular heterogeneity at rest in CAD. Assessment of microvascular heterogeneity offers a potential means for identifying the anatomical and functional significance of CAD without the need for stress.